Results in Engineering 21 (2024) 101801

Contents lists available at ScienceDirect

Results in Engineering

journal homepage: www.sciencedirect.com/journal/results-in-engineering

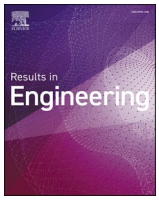

Investigation of the temporal behavior of desiccant disk for use in dehumidifiers and air conditioners

Panos Sphicas [a,*], Apostolos Pesyridis [b,c]

[a] Department of Mechanical Engineering, School of Engineering, University of Birmingham, Dubai International Academic City, P.O. Box 341799, Dubai, United Arab Emirates
[b] Department of Mechanical and Aerospace Engineering, College of Engineering, Design and Physical Sciences, Brunel University London, Uxbridge, UB8 3PH, United Kingdom
[c] Department of Mechanical Engineering, Prince Mohammad Bin Fahd University, Al Khobar, Saudi Arabia

ARTICLE INFO

Keywords:
Air treatment
Cooling
Dehumidification
Waste heat
Solar
Desiccant

ABSTRACT

The majority of household energy is consumed in heating and air conditioning. Desiccant disks are a way to harvest renewable solar energy or waste heat for air conditioning. In the literature there is a gap in the investigation of start-up of desiccant dehumidifiers, which this paper attempts to covers. For this work, a desiccant disk was designed, manufactured, and tested. To reduce the cost, off-the-shelf components were used as structure materials. And as adsorption material, widely available materials were used. Input heat was simulated by an electrical heater and power to auxiliary motors was provided in the form of DC power. Temperature and humidity were recorded at various locations using DHT11 sensors. The system was turned off and tested at a start of operation mode. The performance of the desiccant disk was quantified by the coefficient of performance and the dehumidification efficiency. Results showed gradual increase of the desiccant disk efficiency with a maximum COP value of 0.4 reached within 10 min of the start of operation. Time delays were attributed to heating of the disk. Further work is required to fully understand the transient operation.

1. Introduction

The majority of the energy consumed in a household is directed to heating and air conditioning (Dikshit et al.). Typically dehumidification is based on cooling and compression technologies, which are very energy demanding and utilize harmful to the environment chlorofluorocarbons (CFC) and hydrochlorofluorocarbons (HCFC) [1].

With increasing fuel prices and environmental concerns, renewable energy technologies are developing. However, the main focus of these technologies is the production of electricity. Using the electricity produced by renewable sources for heating and air conditioning creates inefficiencies if the renewable source can be directly used for the purpose of heating and air conditioning [2].

It is well known that the highest load on the electricity generation system is imposed by air conditioners during the warm season. Typically, the sun irradiance experiences a maximum during the warm season. There are several methods to harvest the solar energy for refrigeration purposes. Since the 1990s adsorption technology is used in dehumidification. The National Renewable Energy laboratory has identified thousands of cycles since the early 90s [3]. Upon dehumidification, evaporative coolers are used to cool the process air. Desiccant air conditioning is either liquid-vapor or solid vapor. Liquid–vapor adsorption systems are bulky in size and require a costly pump which consumes a lot of energy. The disadvantages of liquid–vapor adsorption systems are overcome by using solid–vapor cycles [2]. Solid desiccant materials are more compact, cheaper, less corrosive and can handle higher and more sudden loads than liquid desiccants [1]. The capacity for moisture removal is limited by the volume of the solid desiccant. Solid desiccants have low effectiveness in dry climates and periodically the desiccant material needs to be replaced.

Solid desiccants are arranged either in a rotating disk or a twin tower structure. In the twin tower structure, one tower is used to dehumidify the processed air, while the other tower is regenerated. To avoid the complexity, cost and size involved with the twin tower arrangement, this work developed a rotating disk apparatus.

A typical dehumidification disk has the property of absorbing humidity. The disk operates on the principal of Fig. 1. The disk rotates between two partitions: the re-generation partition, and the dehumidifying partition. In the regeneration partition, hot regeneration air is used

* Corresponding author.
E-mail address: p.sphicas@bham.ac.uk (P. Sphicas).

https://doi.org/10.1016/j.rineng.2024.101801
Received 9 December 2023; Received in revised form 11 January 2024; Accepted 13 January 2024
Available online 18 January 2024

Nomenclature

COP	Coefficient of Performance
h	enthalpy [kJ/kgK]
$\dot{m}$	mass flowrate [kg/s]
P_C	Pressure [bar]
T	Temperature [K]
X	Mixing ratio [g/kg]

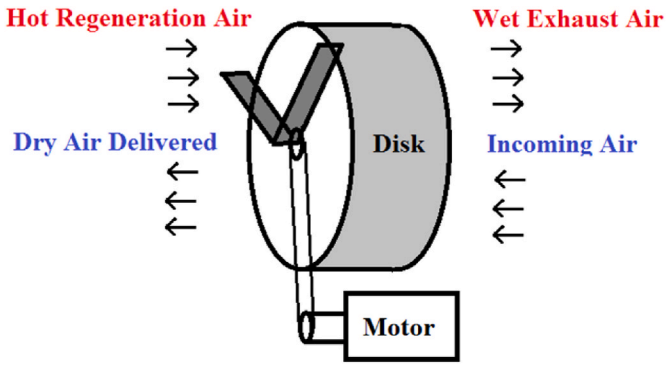

Fig. 1. Schematic of the desiccant disk operation.

to dry a revolving disk. Waste heat or low temperature heat, for example solar, can be used to regenerate/dry the disk. In the literature even hot air from conventional AC units has been utilized for regeneration of the desiccant disk [4]. After drying the disk, the wet exhaust air is disposed of. On the dehumidification partition, incoming air is passed through the disk. The disk will absorb humidity from the air and the dry air will be delivered to the air-conditioned room. If additional cooling is re-quired, water can be sprayed in the dry air for evaporative cooling before the dry air is delivered to the air-conditioned room [5].

Several arrangements of desiccant disks have been proposed in the literature. For example San and Jiang experimented with a double desiccant disk apparatus and regeneration air at 65, 75 and 85 °C [6]. Joudi and Madhi used directly solar energy to regenerate the desiccant [7]. Pramuang used solar parabolic collectors to regenerate silica gel [8]. Ybyraiymkul suggested using distributed microwaves to regenerate silica gel [9]. Several ways to quantify their efficiency have been suggested [5,10]. Table 1 presents a summary of selected publications related to single stage, silica gel desiccant disks. But there is a lack in the literature for the study of their start of operation behavior. Start of operation and transient operation are of particular interest to manufacturers.

For this work, a solid-vapor system was developed. In particular, a water absorption and emission disk was designed, manufactured and tested. Special focus was given in minimizing the cost of production by using widely available materials. The disk was tested at a start of operation mode.

Table 1
Summary of selected publications related to single stage, silica gel desiccant disks.

Authors	Summary	Arrangement	Material
[11]	After many simulations the optimum wheel speed was found	Single Stage	Silica Gel
[8]	Used solar parabolic collectors to regenerate silica gel	Linear	Silica Gel
[12]	Improved the dehumidifying performance by changing the neutralizing agents.	Single Stage	Silica Gel
[13]	Experimental study on the performance of a single stage, silica gel disk	Single Stage	Silica Gel
[14]	Experimentally optimized the geometry of the desiccant disk and the combination of silica gel material	Single Stage	Silica Gel
[15]	CFD simulation of flow and humidity around the desiccant	Single Stage	Silica Gel
[16]	A comprehensive review	Single Stage	Silica Gel

2. Experimental setup

Fig. 2 presents a photograph of the apparatus. The disk is enclosed in a cylindrical shell. A shaft is visible at the front of the apparatus, this shaft is connected to the disk. The shaft is mounted on stainless steel bearings mountain on the apparatus housing. The shaft is driven by an electric motor mounted on the front right leg of the stand on which the shell is secured. The motor is controlled by a motor control resting on the table in front of the apparatus. The top semicircle of the shell is not covered, this section of the disk is used for regeneration. So wet exhaust air is released into the atmosphere. The bottom semicircle is covered by a plate. Two flexible circular tubes are visible at the bottom of the shell, these are used for the incoming air and the dry air.

Combined humidity and temperature sensors, type DHT11, were used. These sensors generate an 8-bit calibrated digital output. The typical accuracy of the measured temperature and humidity is ±5 % RH and ±2 °C respectively. Detailed information about the sensor performance can be found on the datasheet available at ("DHT11 Humidity & Temperature Sensor,"). Table 2 shows the numbering and the location of the installed sensors. All sensors were installed 20 cm away from the disk, to avoid interference from the disk rotation.

An Arduino Uno microcontroller board was used to acquire the signal from the humidity and temperature sensors. The Arduino Uno is based on the ATmega328 P microchip, which allows for the parallel monitoring of 14 8-bit channels at 16 MHz. The Arduino board was powered by a USB connection, which was also used to transfer data. The data from the Arduino board were fed to a typical Windows 10 intel i7 laptop at a frequency of 0.4 Hz.

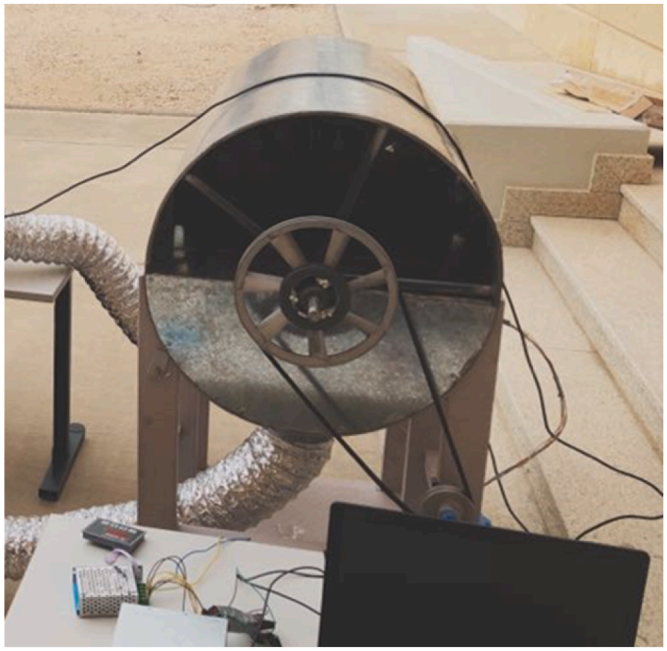

Fig. 2. Photograph of the desiccant disk apparatus.

Table 2
Location of the installed DHT11 sensors.

Sensor Number	Location of Sensor
1	Entrance of regeneration "Hot Regeneration Air"
2	Exit of regeneration "Wet exhaust air"
3	"Delivered Dry Air"
4	"Incoming Air"
5	Ambient

3. Material characterization

An important design factor of the desiccant disk is the absorption and regeneration performance of the absorption material. The material used in this work is silica gel supplied by "Dry&Dry", in beads ranging in size between 3 and 5 mm. The material has a purity of 98.2 % amorphous silica and contains up to 0.2 % activated coloring agent. Silica gel was chosen due to its high moisture adsorption capacity [17]. Fig. 3 presents the filling of the apparatus with the desiccant material. To characterize the material, the rig of Fig. 4 was built. As shown, it consists of a tube filled with the absortption material and caped on both sides by mesh. The cylinder was placed on a precision scale and air was supplied through the mesh.

To characterize the absorption of the material, the material was initially fully dried and steam was supplied to the cylinder of Fig. 4. The steam increased the absorbed humidity. The weight and elapsed time were constantly recorded. Gradually the mate-rial was brought to complete saturation.

To characterize the regeneration of the material, the material was initially fully saturated and dry hot air was supplied to the cylinder of Fig. 4. The dry hot air, re-duced the absorbed humidity. The weight and elapsed time were constantly recorded. Gradually the material was fully dried.

The absorption properties of the material used in this work is presented in Fig. 5. For low levels of water content, the material appears to absorb water at a slightly higher temporal rate. With increasing level of water content, the temporal rate of absorbion reduces until saturation is met. The material was fully surrounded by water vapor at 100 °C and it took approximately 300 s to reach full saturation. The time required for full saturation is an important design parameter for the desiccant disk and the rotational speed.

Fig. 6 shows the regeneration properties of the material used. At full water-saturation of the material, the regeneration occurs at the highest temporal rate. As the water content of the material reduces, so does the rate of regeneration, reaching a plateau of the humidity of the regeneration air.

Fig. 3. Filling of the desiccant disk with the material.

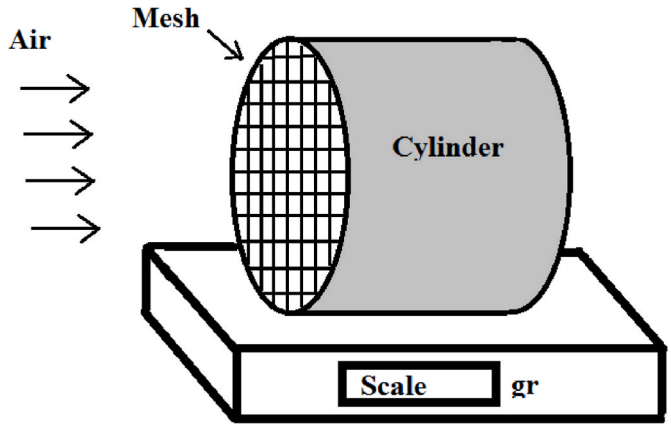

Fig. 4. Custom-made rig for characterization of the material absorption properties.

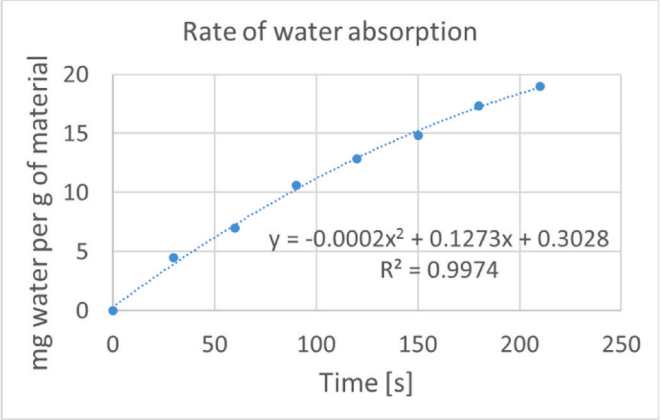

Fig. 5. Rate of water absorption.

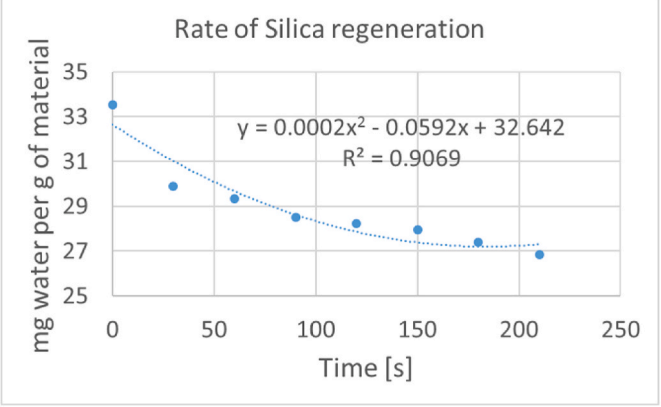

Fig. 6. Rate of regeneration.

4. Discussion

A custom built, 27-m3 wooden room, was used to simulate the air-conditioned room. In the room, a 2-kw kettle was left boiling, simulating a heat and humidity load. The "dry air delivered" was delivered in

the room. Also, the "incoming air", was pumped from the same wooden room, exactly as a typical dehumidifier would operate.

Three independent tests, each lasting 20 min, were performed on the same day. The time interval between the tests was approximately 20 min. During the time interval, the room door was left open, to allow equilibrium with the ambient environ-ment. At the beginning of every test the disk was dry from previous use, as it would be under normal, intermittent operation.

The recording of the three tests were ensemble averaged, to filter out random fluctions and discrepancies between the tests. Sensor 5 refers to the ambient conditions, which were averaged to 60 % relative humidity and 23.5 °C.

For the different sensors described in Table 2, the recorded temperature is shown in Figs. 7 and 9, and the recorded relative humidity in Fig. 8. The figures, pre-sent the ensemble averaged recordings as described earlier. It was observed that the system required about 10 min to reach steady state, so only the first 10 min after the start of operation are presented.

In Fig. 7, sensor 1, which records the temperature of the "Hot Regeneration Air", measures an increase in temperature after the start of operation. This is the effect of the heat delivered to the desiccant disk by the electrical heater. The long-term scope of the project is to have heat delivered by solar or waste heat sources. But currently, the elec-trical heater simulates the heat source. The increased temperature, reduces the relative humidity, as in warmer air, more water can be dissolved. The mixing ratio, also known as specific humidity, which is the ratio of mass of water to mass of air, remains the same. The heat source does not alter the water content of air.

In Fig. 7, the "Hot Regeneration Air", is the highest temperature recorded. This is normal, as the hot regeneration air is the highest temperature in the cycle. After the start of operation, it takes approximately 7 min for the air to reach the plateau temperature of 50 °C. This is a reasonable amount of time for the hot regeneration air pipes to warm up. Sensor 2 refers to the "wet exhaust air", which also warms up, but with a time phase difference to the temperature of the hot regeneration air. The rec-orded time difference is expected, as sensor 2 is located downstream of sensor 1, after the desiccant disk. The desiccant disk requires time to reach steady state, due to its ro-tation and convective cooling from the "incoming air". Sensor 2, records a maximum of about 45 °C, which is about 5 °C lower than the "hot regeneration air". The heat losses from the hot regeneration air are directed to warming up the desiccant disk, the "dry air delivered", and the environment.

Fig. 8 shows an almost immediate reduction in the mixing ratio from the am-bient recorded 5 g of water per kg of dry air to 4.2 g/kg. This is the effect of two mecha-nisms. Firstly, in this setup, the dry delivered air was sent to a wooden box, which simulated a room of dimensions 27 m3.

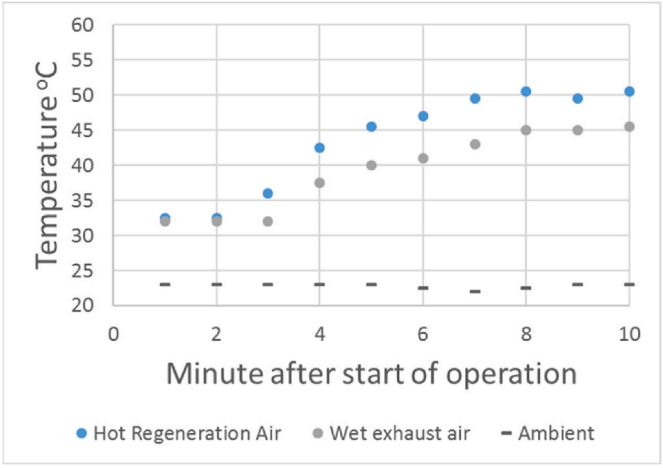

Fig. 7. Recorded temperature on regeneration partition.

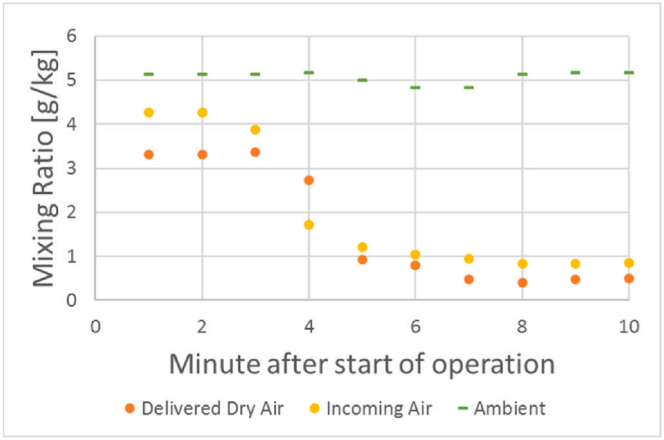

Fig. 8. Recorded relative humidity on the dehumidifying partition.

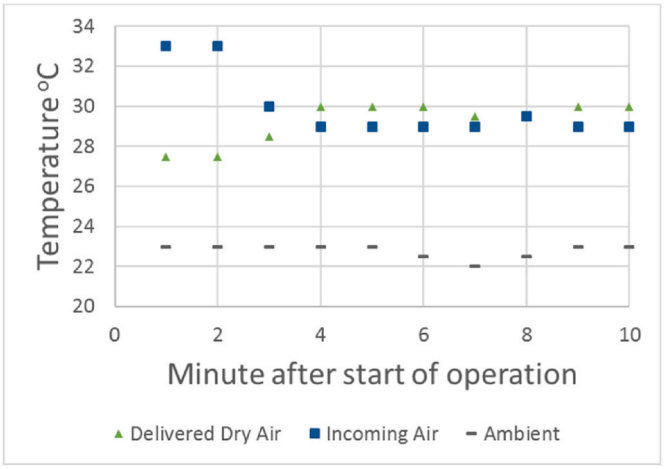

Fig. 9. Recorded temperature on dehumidifying partition.

The incoming air, was then pumped from the same wooden room, as a typical dehumidifier would operate. Before every test, the room door was left open for the air to reach ambient conditions. However, the air in the cylinder and pipes is trapped. Once the operation of the desiccant disk begins, the trapped air of lower humidity and higher temperature will affect the measurements. Secondly, like in a real life application, the desiccant disk is dry prior to start of opera-tion and the desiccant disk absorbs humidity from the incoming air. As a result, even the very initial readings of the dry delivered air will show a lower mixing ratio than ambient.

Fig. 9 demonstrates an unwanted phenomenon in the operation of such desic-cant disks. At the end of the regeneration part, the disk is hot from the hot regeneration air, this heat will be transferred to the dehumidified air. Warming up the delivered dry air is not wanted. To avoid this problem, many researchers have add a small purging section between the regeneration partition and the dehumidification partition. Typically 5–10 % of the dehumidified air is used to purge the desiccant disk [18].

The desiccant disk operates as a heat capacitor and transfers heat from the hot re-generation air to the dry delivered air. Sensor 3 captures this trend and an increase in temperature is observed. Initially the delivered dry air has a temperature of 27 °C, which is close to the ambient recorded temperature of 23 °C. But after about 10 min, the delivered dry air temperature has risen to about 30 °C. On the other hand, sensor 4, which records the incoming air temperature, records an initial increase of temperature, attributed to the kettle in the room, but afterwards reaches a steady state temperature at about 29 °C. It must be

noted that both sensors 3 and 4 record temperature higher than ambient (sensor 5).

The performance of the desiccant disk can be quantified using the Coefficient of Performance (COP). For this work, the COP is calculated as:

$$COP = \frac{\dot{m}_{dehymidying}(h_3 - h_4)}{\dot{m}_{regeneration}(h_1 - h_2)} \quad (1)$$

Where $\dot{m}_{dehymidying}$ is the process dehumidified air mass flow rate and $\dot{m}_{regeneration}$ is the hot regeneration air mass flow rate. The enthalpies h_1 to h_4 refer to the enthalpies of the sensors, as numbered in Table 2.

The enthalpy was calculated from the measured temperatures using the empirical expressions derived by Ref. [18]. These formulas give the water vapor saturation pressure to sufficient accuracy between 0 °C and 373 °C, which is a range sufficient for this application.

$$\ln\left(\frac{P_{ws}}{P_C}\right) = \frac{T_c}{T}\left(C_1\vartheta + C_2\vartheta^{1.5} + C_3\vartheta^3 + C_4\vartheta^{3.5} + C_5\vartheta^4 + C_6\vartheta^{7.5}\right) \quad (2)$$

$$\vartheta = 1 - \frac{T}{T_c} \quad (3)$$

Where T is the temperature, P_{ws} the water vapor saturation pressure, T_c the critical temperature and P_C the critical pressure. Temperature is expressed in K and pressure in hPa. The critical temperature of water is 647.096 K and the critical pressure of water is 220 640 hPa. The coefficients C_1 to C_7 have known values.

The mixing ratio (mass of water vapor over mass of dry gas) in g/kg is calculated as:

$$X = B \bullet P_w / (P_{tot} - P_w) \quad (4)$$

B is a constant, whose value depends on the gas, it can be calculated as:

$$B = MW(H_2O) / MW(gas) \bullet 1000 \quad (5)$$

$MW(H_2O)$ is the molecular weight of water and $MW(gas)$ is the molecular weight of the carrier gas, in this case air. For air, the value of B is 621.9907 g/kg.

From the definition of RH, the water vapor pressure can be written as:

$$P_w = P_{ws} \bullet RH/100 \quad (6)$$

Finally, the enthalpy h of the wet air in kJ/kg can be calculated from the mixing ratio as:

$$h = T \bullet (1.011 + 0.00189 \bullet X) + 2.5 \bullet X \quad (7)$$

where T is the temperature in °C.

Fig. 10 shows the temporal evolution of the coefficient of performance of the desiccant disk after the start of operation. Initially, the COP is very low, indicating that the overall efficiency of the system after start of operation is very low. As time lapses, the dry delivered air in the room, is pumped into the desiccant disk again, increasing the performance of the system. Gradually the system reaches steady state and so does the COP at about 10 min after start of operation.

However, the coefficient of performance is based on the ration of enthalpy differences. A more practical definition of efficiency is the dehumidification efficiency $n_{deh} = \frac{X_4 - X_3}{X_4}$. The dehumidification efficiency represents the humidity reduction across the desiccant disk, over the humidity of the incoming air. For the calculation of this efficiency, the temperature of air needs to be removed as a parameter. So, the mixing ratio is used for the calculation of the dehumidification efficiency.

Fig. 11 presents the dehumidification efficiency as a function of time after start of operation. The dehumidification efficiency starts at a value of approximately 0.2. For the first few minutes, the efficiency fluctuates around the value of 0.2. This fluctuation is contributed to initialization of the desiccant material and measuring fluctuation. The dehumidification efficiency gradually increases to 0.5 at about 10 min after the start of operation.

5. Conclusions

A solid-vapor desiccant disk was designed and manufactured. The design tried to minimize cost. Air temperature and relative humidity was measured at different locations of the setup. The temporal response of the disk, at the start of operation, was investigated. The hot regeneration air and the wet exhaust air both experienced an increase in temperature, but with a time delay between them, attributed to the warming of the disk. The delivered dry air and the incoming air both experienced a reduction in humidity, but with a time delay, attributed to the recirculation of the dry air delivered in the room. Also, the temporal performance of the disk was quantified with the coefficient of performance COP and the dehumidification efficiency n_{deh}. Both efficiencies showed a gradual increase for the first 10 min until the system reached steady state. Desiccant disk dehumidification technology seems promising, but further work is needed to fully understand transient operation and long-term aging on the solid desiccant.

CRediT authorship contribution statement

Panos Sphicas: Project administration, Methodology, Investigation, Funding acquisition, Formal analysis, Data curation, Conceptualization. **Apostolos Pesyridis:** Writing – review & editing, Supervision.

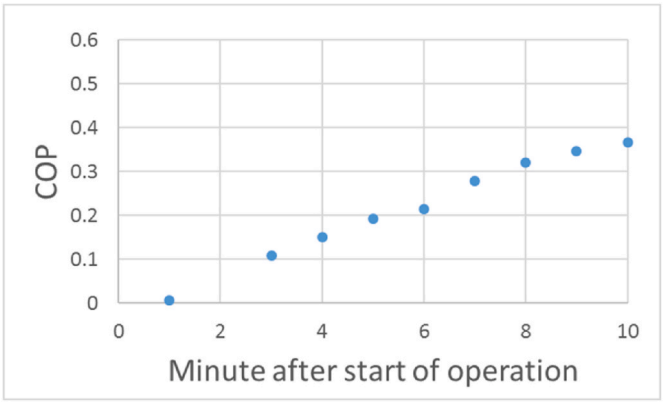

Fig. 10. Coefficient of Performance of desiccant disk.

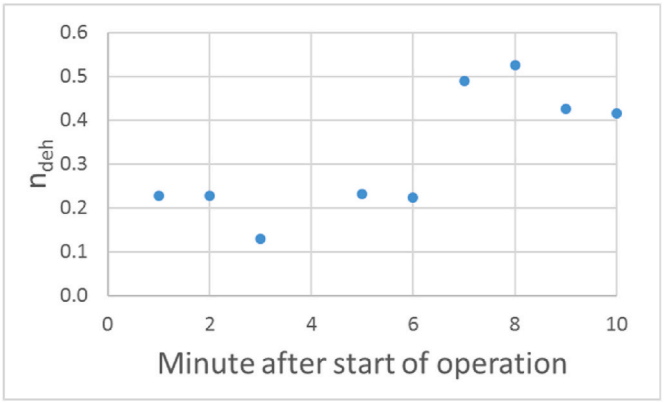

Fig. 11. Dehumidification effectiveness of desiccant disk.

Declaration of competing interest

The authors declare that they have no known competing financial interests or personal relationships that could have appeared to influence the work reported in this paper.

Data availability

Data will be made available on request.

References

[1] K.S. Rambhad, P.V. Walke, D.J. Tidke, Solid desiccant dehumidification and regeneration methods—a review, Renew. Sustain. Energy Rev. 59 (2016) 73–83, https://doi.org/10.1016/j.rser.2015.12.264.

[2] K.R. Ullah, R. Saidur, H.W. Ping, R.K. Akikur, N.H. Shuvo, A review of solar thermal refrigeration and cooling methods, Renew. Sustain. Energy Rev. 24 (2013) 499–513, https://doi.org/10.1016/j.rser.2013.03.024.

[3] A.A. Pesaran, T.R. Penney, A.W. Czanderna, Desiccant Cooling: State-Of-The-Art Asessment, 1992.

[4] T. Hussain, Optimization and comparative performance analysis of conventional and desiccant air conditioning systems regenerated by two different modes for hot and humid climates: experimental investigation, Energy and Built Environment 4 (3) (2023) 281–296, https://doi.org/10.1016/j.enbenv.2022.01.003.

[5] D.B. Jani, M. Mishra, P.K. Sahoo, Solid desiccant air conditioning – a state of the art review, Renew. Sustain. Energy Rev. 60 (2016) 1451–1469, https://doi.org/10.1016/j.rser.2016.03.031.

[6] J.-Y. San, G.-D. Jiang, Modeling and testing of a silica gel packed-bed system, Int. J. Heat Mass Tran. 37 (8) (1994) 1173–1179, https://doi.org/10.1016/0017-9310(94)90203-8.

[7] K.A. Joudi, S.M. Madhi, An experimental investigation into a solar assisted desiccant-evaporative air-conditioning system, Sol. Energy 39 (2) (1987) 97–107, https://doi.org/10.1016/S0038-092X(87)80037-3.

[8] S. Pramuang, R.H.B. Exell, The regeneration of silica gel desiccant by air from a solar heater with a compound parabolic concentrator, Renew. Energy 32 (1) (2007) 173–182, https://doi.org/10.1016/j.renene.2006.02.009.

[9] D. Ybyraiymkul, Q. Chen, M. Burhan, F.H. Akhtar, R. AlRowais, M.W. Shahzad, M. K. Ja, K.C. Ng, Innovative solid desiccant dehumidification using distributed microwaves, Sci. Rep. 13 (1) (2023) 7386, https://doi.org/10.1038/s41598-023-34542-9.

[10] G. Angrisani, C. Roselli, M. Sasso, Effect of rotational speed on the performances of a desiccant wheel, Appl. Energy 104 (2013) 268–275, https://doi.org/10.1016/j.apenergy.2012.10.051.

[11] S. De Antonellis, C.M. Joppolo, L. Molinaroli, Simulation, performance analysis and optimization of desiccant wheels, Energy Build. 42 (9) (2010) 1386–1393, https://doi.org/10.1016/j.enbuild.2010.03.007.

[12] T. Kuma, T. Hirose, Performance of honeycomb rotor dehumidifier in improved methods of adsorbent preparation, J. Chem. Eng. Jpn. 29 (1996) 376–378.

[13] U. Hanifah, M.A. Karim, A. Haryanto, R. Alfiyah, A. Taufan, Experimental performance of A rotary desiccant wheel without honeycomb matrix structure: a preliminary study, IOP Conf. Ser. Mater. Sci. Eng. 1096 (1) (2021) 012043, https://doi.org/10.1088/1757-899X/1096/1/012043.

[14] K.S. Rambhad, P.V. Walke, V.P. Kalbande, M.A. Kumbhalkar, V.W. Khond, Y. Nandanwar, M. Mohan, R. Jibhakate, Experimental investigation of desiccant dehumidification with four different combinations of silica gel desiccant wheel on indoor air quality, SN Appl. Sci. 5 (11) (2023) 277, https://doi.org/10.1007/s42452-023-05505-6.

[15] J. Taweekun, V. Akvanich, The experiment and simulation of solid desiccant dehumidification for air-conditioning system in a tropical humid climate, Engineering 5 (1A) (2013) 146–153, https://doi.org/10.4236/eng.2013.51A021.

[16] S.V. Dikshit, S. Chavali, P.D. Malwe, S. Kulkarni, H. Panchal, A.J. Alrubaie, M. Mohamed, M.M. Jaber, A comprehensive review on dehumidification system using solid desiccant for thermal comfort in HVAC applications, Proc. Inst. Mech. Eng., Part E: J. Process Mech. Eng. (2023) 095440892311630, https://doi.org/10.1177/09544089231163024.

[17] L.-Z. Zhang, H.-X. Fu, Q.-R. Yang, J.-C. Xu, Performance comparisons of honeycomb-type adsorbent beds (wheels) for air dehumidification with various desiccant wall materials, Energy 65 (2014) 430–440, https://doi.org/10.1016/j.energy.2013.11.042.

[18] W. Wagner, A. Pruss, The IAPWS formulation 1995 for the thermodynamic properties of ordinary water substance for general and scientific use, J. Phys. Chem. Ref. Data 31 (2002) 387–535.